

# Physics and applications of laser diode chaos

M. Sciamanna<sup>1\*</sup> and K. A. Shore<sup>2</sup>

This Review Article provides an overview of chaos in laser diodes by surveying experimental achievements in the area and explaining the theory behind the phenomenon. The fundamental physics underpinning laser diode chaos and also the opportunities for harnessing it for potential applications are discussed. The availability and ease of operation of laser diodes, in a wide range of configurations, make them a convenient testbed for exploring basic aspects of nonlinear and chaotic dynamics. It also makes them attractive for practical tasks, such as chaos-based secure communications and random number generation. Avenues for future research and development of chaotic laser diodes are also identified.

The emergence of irregular pulsations and dynamical instabilities from a laser were first noted during very early stages of the development of lasers. Pulses with an amplitude that “varies in an erratic manner” were reported in the output of the ruby solid-state laser<sup>1</sup> (Fig. 1a) and then found in numerical simulations<sup>2</sup>. However the lack of knowledge of what would later be termed chaos resulted in these initial observations being either left unexplained or wrongly attributed to noise.

The situation changed in the late 1960s with the discovery of sensitivity to initial conditions by Lorenz<sup>3</sup>, later popularized as the ‘butterfly effect’. As illustrated in Fig. 1b, numerical simulations of a deterministic model of only three nonlinear equations showed an irregular pulsing with a remarkable feature: the state variables evolve along very different trajectories despite starting with approximately the same initial values. The distance as a function of time,  $\delta(t)$ , between nearby trajectories diverges exponentially according to  $\delta(t) = \delta(0)\exp(\lambda t)$ , provided that  $\lambda$ , the effective Lyapunov exponent of the dynamical system, is positive. Consequently, such systems are unpredictable in the long term. Plotted in the  $x$ - $y$ - $z$  phase space of the state variables, the trajectories converge to an ‘attractor’ that has the geometric property of being bounded in space despite the exponential divergence of nearby trajectories (Fig. 1c). Such attractors are found to have a fractional dimension<sup>4</sup> and are thus termed strange. Aperiodicity, sensitive dependency to initial conditions and strangeness are commonly considered as the main properties for chaos<sup>5</sup>. Numerous practical algorithms are available today to differentiate between deterministic chaos and stochastic noise, including estimating the dominant positive Lyapunov exponent<sup>6</sup> and the fractal dimension<sup>7</sup>, as illustrated in Fig. 1d and Fig. 1e, for Lorenz chaos.

The fields of laser physics and chaos theory developed independently until 1975<sup>8</sup> when Haken discovered a striking analogy between the Lorenz equations that model fluid convection and the Maxwell–Bloch equations modelling light–matter interaction in single-mode lasers. The nonlinear interaction between the wave propagation in the laser cavity (represented by the electric field,  $E$ ) and radiative recombination producing macroscopic polarization (encapsulated in the polarization,  $P$ , and the carrier inversion,  $N$ ) yield similar dynamical instabilities to those found in the Lorenz equations. More specifically, in addition to the conventional laser threshold, Haken<sup>8</sup> suggested a second threshold would exist above which “spiking occurs randomly though the equations are completely deterministic”.

Motivated by the new theoretical developments of chaos theory<sup>9–11</sup>, laser experimentalists started an intense search for Lorenz–Haken chaos. However, Haken’s second threshold requires a high-loss

resonator and pumping the laser at about 10–20 times the first laser threshold. In addition, although the Lorenz and laser Maxwell–Bloch equations share many similar dynamical properties, the parameters that determine the relaxations of the state variables in both physical systems take very different values. In particular, in some lasers the polarization and/or the carrier inversion relax much faster than the field and thus can be adiabatically eliminated from the other equations, hence reducing the system’s dimension. The first conclusive experimental reports of laser chaos were therefore obtained in a CO<sub>2</sub> laser where loss modulation provides the additional degrees of freedom to achieve chaotic trajectories<sup>12,13</sup>. Lorenz–Haken chaos in a free-running laser was only achieved later in an 81.5 μm NH<sub>3</sub> laser<sup>14</sup>, in which low pressure and long wavelength combine to reduce the secondary laser threshold (Fig. 1f).

## The laser diode as a damped nonlinear oscillator

These early demonstrations motivated investigations in more practical lasers such as laser diodes. Laser diodes have numerous applications including imaging, sensing, fibre-optic communications and spectroscopy. Initially aimed at providing a constant output power, laser diodes are today commonly used to produce periodical short optical pulses at high repetition rates<sup>15</sup>. Besides steady operation and pulsing dynamics, chaos theory reveals that a nonlinear physical system of high enough dimension may bifurcate to more complex dynamics including chaos. This applies also to laser diodes. However, in considering the analogy with Lorenz chaos, it must be appreciated that in laser diodes the polarization typically relaxes much faster (at a rate of  $\gamma_p$ ) than the field (at a rate of  $\kappa$ ) and the carrier inversion (at a rate of  $\gamma_N$ ), that is,  $\gamma_p \gg \kappa > \gamma_N$  (ref. 16). As a result, laser diode dynamics is described using rate equations for the field and carrier inversion as a driven damped nonlinear oscillator and is therefore limited to a spiralling flow towards a steady-state (so-called relaxation oscillations; Fig. 1g). However, laser diodes, almost uniquely, possess a property that makes them extremely sensitive to optical perturbations: their emission frequency is detuned from the gain spectrum peak leading to an anomalous dispersion effect at the lasing frequency. This property results in a refractive index variation with carrier density and translates into a so-called  $\alpha$ -factor that explains laser chirp and linewidth broadening<sup>17</sup>, but also facilitates laser instabilities<sup>18,19</sup>.

In this Review Article we review situations in which a laser diode can be brought into chaos and then describe currently identified applications of laser diode chaos. Finally we offer reasons for our expectation that this area of activity will remain a fertile field for future research.

<sup>1</sup>CentraleSupélec, Laboratoire Matériaux Optiques, Photonique et Systèmes (LMOPS) (CentraleSupélec/Université de Lorraine) and Optics and Electronics (OPTEL) Research Group, 2 Rue Edouard Belin, 57070 Metz, France. <sup>2</sup>Bangor University, School of Electronic Engineering, Dean Street, Bangor LL57 1UT, UK. \*e-mail: marc.sciamanna@centralesupelec.fr

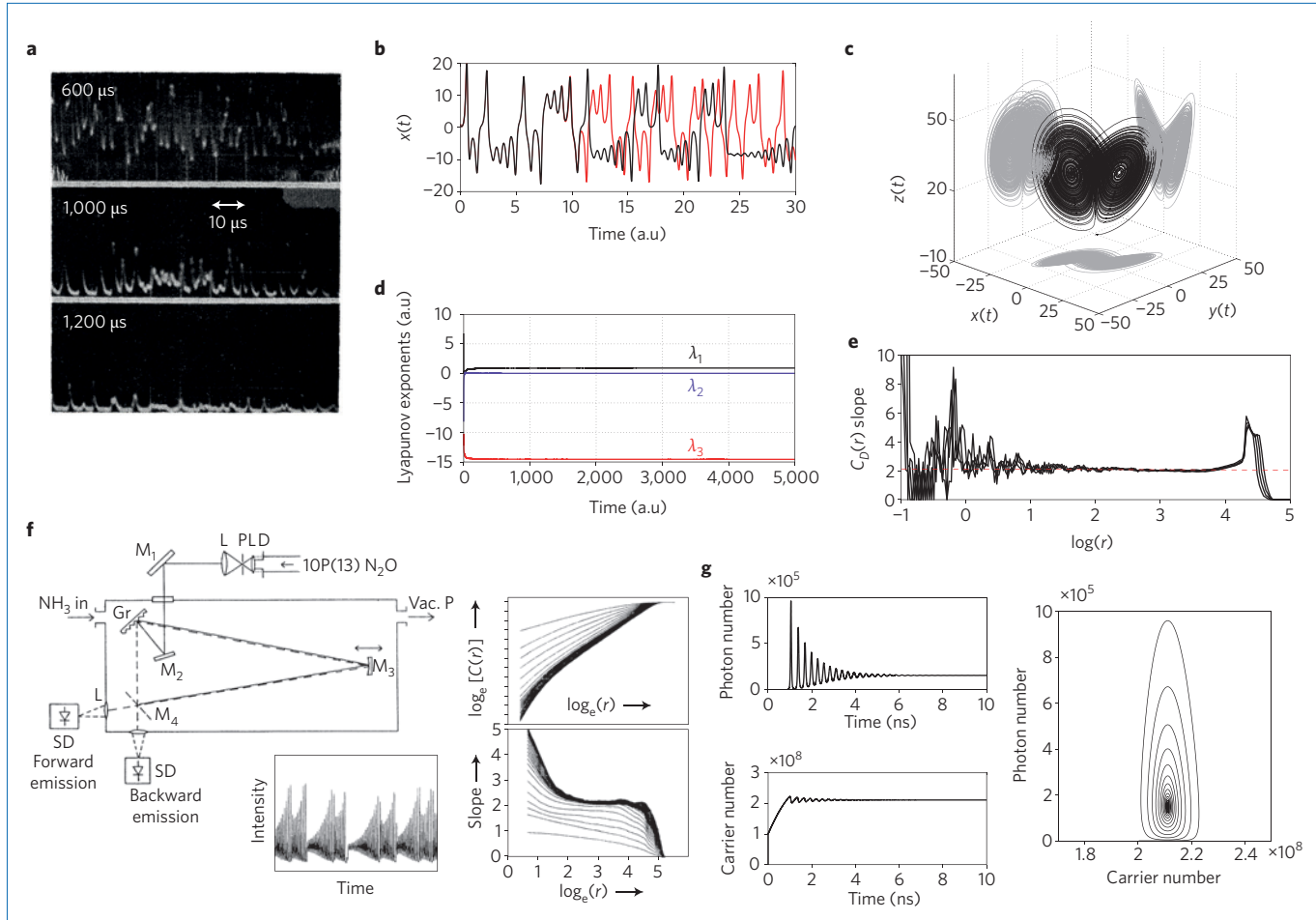


**Figure 1 | Chaos properties and chaos in lasers.** **a**, The irregular pulsing dynamics observed in the output of the ruby solid-state laser. Reproduced from ref. 1, APS. **b–e**, Numerical simulation of Lorenz chaos. The Lorenz equations (ref. 3) are three nonlinear differential equations for the variables  $x$ ,  $y$  and  $z$  with parameters  $r$ ,  $b$  and  $\sigma$ . We have fixed the values of the parameters:  $r = 28$ ,  $b = 8/3$ ,  $\sigma = 10$ . **b**, Time-traces of  $x$  for two slightly different initial conditions (black and red trajectories). **c**, Trajectories in the three-dimensional phase space (black) with projections in the two-dimensional phase planes (grey). **d**, Computation of the three Lyapunov exponents,  $\lambda_i$ , using the Wolf algorithm<sup>6</sup> for the dynamics in **b**. The dynamics shows one positive Lyapunov exponent,  $\lambda_1$ . **e**, Computation of the correlation dimension,  $D$ , using the Grassberger-Procaccia algorithm<sup>7</sup>, which measures the dimensionality of the space occupied by a set of points. The algorithm computes the correlation integral,  $C(r)$ , for increasing distance  $r$  between points and for increasing embedding dimension. For a large enough embedding dimension and in a given range of  $r$ ,  $C(r)$  scales as  $C(r) = r^D$  where  $D$  is the correlation dimension that is a lower bound estimation of the fractal dimension. The red dashed line corresponds to  $D \sim 2.05$ . **f**, Experimental observation of Lorenz chaos in a free-running  $\text{NH}_3$  laser.  $M$ , mirror;  $Gr$ , grating;  $L$ , lens;  $SD$ , Schottky-barrier diode;  $P$ , pinhole diaphragm;  $D$ , diaphragm. Bottom panel: typical time-trace of the pulsating intensity. Right panel: computation of the correlation dimension from the experimental time-series. Reproduced from ref. 131, APS. **g**, Simulated dynamics of a laser diode with an injection current step. The photon number and carrier inversion show damped oscillations towards a steady-state (relaxation oscillations). Right panel: dynamics is limited to spiralling relaxation flows in the phase plane.

### Configurations for achieving laser diode chaos

Several configurations may be used to overcome damped relaxation oscillations and therefore to generate laser diode chaos.

**External optical feedback.** Returning a small fraction of the laser emission into the laser diode cavity may result in a chaotic output with different types of waveforms and properties<sup>20</sup> (Fig. 2a). The richness of the dynamics results from the competition between the laser's intrinsic relaxation oscillation frequency,  $f_{\text{RO}}$ , and the frequency of the external cavity,  $f_{\text{EC}} = c/(2L)$ , where  $c$  is the speed of light and  $L$  is the distance from the laser to the external optical feedback element<sup>21,22</sup>. Chaotic dynamics in the case where  $f_{\text{EC}} \ll f_{\text{RO}}$  include low-frequency power fluctuations<sup>23</sup> or coherence-collapse dynamics<sup>24</sup> typically giving a high-dimensional chaotic attractor<sup>25</sup>. In contrast, for  $f_{\text{EC}} \gg f_{\text{RO}}$ , different self-organizing dynamics take place including periodic pulsing at the external-cavity

frequency<sup>22</sup>, with bifurcations to quasiperiodic dynamics such as regular pulse packages<sup>26</sup>.

The feedback can be provided either from a simple external mirror or with more complex configurations leading to different routes to chaos, for example, feedback from a phase-conjugate mirror<sup>27,28</sup> or including a Fabry-Pérot etalon as a filter in the external cavity<sup>29</sup>. Numerous works have extended the study to multimode laser dynamics by considering, for example, the inclusion of a diffraction grating in the external cavity<sup>30</sup>, or the inclusion of polarizers<sup>31</sup> or retarding plates<sup>32</sup> as ways to influence the polarization of the returning field; thus providing additional ways to select and control specific pulsing or chaotic dynamics<sup>33</sup>.

External optical feedback is the most prominent configuration in applications using laser diode chaos and is commonly used for chaos-based secure communications, random number generation, chaos computing and sensing. The scaling of the time-delay

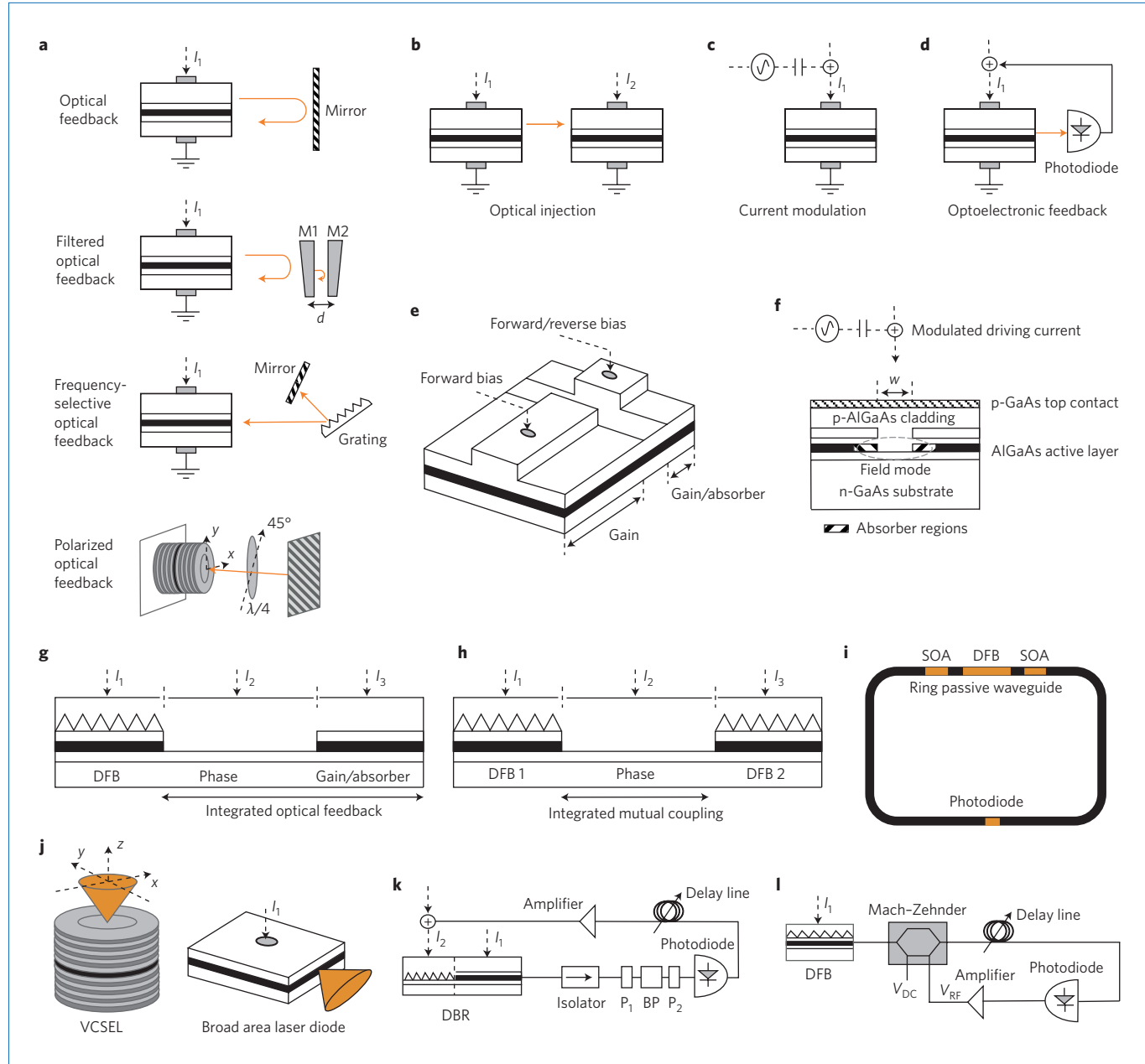


**Figure 2 | Configurations for achieving chaos in laser diode.** **a**, Optical feedback can be provided by an external mirror that reflects light (red arrow) back into the laser diode (top). A Fabry-Pérot etalon defined by two mirrors, M1 and M2, separated by a distance  $d$  provides filtered optical feedback (second from top). A diffraction grating offers mode selectivity (third from top). Polarized optical feedback can be provided, for example, a quarter-waveplate that rotates the polarization of the returning field (bottom). **b**, Optical injection from a master to a slave laser diode. **c**, External current modulation applied to a laser diode. **d**, Optoelectronic feedback by re-injecting a delayed and amplified signal from a photodiode that measures the laser output. **e**, A two-section laser diode with one section working as a gain or a saturable absorber section depending on the applied voltage. **f**, Narrow stripe semiconductor laser with transverse loss modulation.  $w$  is the aperture width. The dashed grey oval shows the extension of the optical field to the unpumped (absorber) regions. **g**, Integrated chaotic laser diode with a passive feedback cavity and a gain/absorber section for adjusting the feedback strength. **h**, Integrated chaotic laser diode using mutual coupling between two DFB laser sections. **i**, Integrated chaotic laser diode with a ring passive cavity. **j**, Chaos resulting from mode competition; either polarization competition in VCSELs or competition between transverse modes in a broad area laser diode. **k**, Wavelength chaos generator using a nonlinear optoelectronic feedback on a DBR laser. A birefringent plate (BP) with two polarizers (P1 and P2) non-linearly converts the incoming intensity. **l**, Intensity chaos generator using nonlinear optoelectronic feedback from a Mach-Zehnder electro-optic modulator.  $I_i$  indicates the application of current  $i$ .

with respect to the laser internal timescale and the sensitivity of the phase to the returning field create a means of inducing various dynamical scenarios leading to chaos<sup>34,35</sup> and of engineering high-dimensional chaotic waveforms spanning a large frequency bandwidth.

**Optical injection.** Optical injection from another laser can also be used to destabilize diode lasers (Fig. 2b). In the case of large frequency detuning and/or strong injection, the injected laser destabilizes to chaos through different bifurcation mechanisms<sup>36,37</sup>. The availability of mathematical continuation techniques that follow bifurcations in

a two-dimensional parameter plane together with the limited set of parameters influencing the nonlinear dynamics has made it possible to reach an unprecedented global agreement between experiment and theory over a large range of injection parameters<sup>37</sup>. By harnessing the nonlinear dynamics of optical injection one can engineer and select dynamics for specific needs. The transition to chaos through period doubling has been used, for example, as a frequency multiplication or conversion process in photonic microwave generation<sup>38</sup> or in remote sensing where an even low-irradiance light injected into the diode laser is detected through the resulting bifurcations<sup>39</sup>. As with optical feedback, injection of either a polarized field or a single mode into a laser emitting in several polarizations<sup>40</sup> or longitudinal mode<sup>41</sup> components leads to new mechanisms for chaos instabilities but simultaneously provides additional ways to control the dynamics.

**External current modulation.** Direct current modulation of a laser diode (Fig. 2c) is a common practice. Less familiar is the opportunity to achieve chaotic pulsing when the modulation frequency is close to the laser relaxation oscillation frequency and/or the modulation depth is relatively large. The first theoretical works suggested a period-doubling route to chaos with increased modulation depth<sup>42</sup>. Experiments, however, showed that the intrinsic noise from quantum fluctuations typically prevents the observation of a period-doubling cascade to chaos<sup>43</sup>, unless there is careful tuning of both the modulation frequency and depth<sup>44</sup>. Recent works have indicated that specific laser diodes such as vertical-cavity surface-emitting lasers (VCSELs), whose dynamics may involve several polarization or transverse modes<sup>45</sup>, display chaos for a much wider range of the modulation parameters.

**Loss-modulation using saturable absorber.** Modulation of the optical losses in the laser resonator can also cause dynamical instabilities. This is typically achieved by combining a gain section with a reverse bias section that behaves as a saturable absorber (Fig. 2e). A noisy spike with an intensity large enough to saturate the absorber will initiate a process of loss-modulation with the periodicity of the round-trip propagation of the pulse—so-called passive mode-locking. Increasing either the reverse bias voltage in the absorber section or the current in the gain section destabilizes the self-pulsing leading to period-doubling (harmonic mode-locking) and then to chaos<sup>46</sup>. Although harmonic passive mode-locking has been observed experimentally<sup>47</sup>, the experimental observation of chaotic pulsing has been limited to two-section quantum-dot laser diodes where the carrier dynamics has additional features<sup>48</sup>.

With a positive bias in both sections, another mechanism for the instability of self-pulsations arises. The laser diode  $\alpha$ -factor couples any change of the differential gain (as induced by a variation of the current) to a change of the refractive index, thus reducing the wavelength detuning between the two sections. When the current in one of the two sections is large enough this detuning cannot be compensated. The system then behaves like two coupled but strongly detuned nonlinear oscillators displaying chaos<sup>49,50</sup>.

Narrow-stripe semiconductor lasers used in optical storage (such as compact-disk lasers) also exhibit self-pulsing instabilities (Fig. 2f). Two blocking layers confine the current injection to the centre of the device, leaving unpumped regions at either side. The penetration of the optical mode into these unpumped regions creates saturable absorption that transversally modulates the optical losses. The so-called Yamada model<sup>51</sup> has clarified the onset of self-pulsation. Chaotic self-pulsations in these devices have been experimentally observed with the addition of external modulation<sup>52</sup> or external optical feedback<sup>53</sup>.

**Optoelectronic feedback.** In optoelectronic feedback the output of the laser diode is first converted to an electrical current by a photodiode before being amplified and re-applied via the laser

driving current (Fig. 2d). In this way, the laser diode experiences a time-delayed contribution to its dynamics. The feedback signal is termed incoherent because it only interacts with the carriers. The feedback may be positive or negative depending on the polarity of the amplifier in the feedback loop. Nonlinear dynamics typically arise when the time-delay is larger than the laser relaxation oscillation time-period. Experiments have captured regular pulsing dynamics but also quasiperiodic bifurcations to chaos when varying the time-delay and/or the feedback strength<sup>54</sup>. The parameter region displaying chaos is wider in the case of negative optoelectronic feedback<sup>55</sup>.

**Integrated on-chip chaotic laser diode.** Several proposals have been made for integrating optical feedback leading to on-chip chaotic laser diodes. Three-contact laser diodes have been developed integrating a distributed feedback (DFB) lasing section with a gain or absorber section and a passive waveguide providing integrated optical feedback with a short external cavity (200  $\mu\text{m}$ )<sup>56</sup> (Fig. 2g). The current driving the gain/absorber section enables control of the feedback strength, whereas the current driving the passive waveguide is used for adjusting the feedback phase. Both a quasiperiodic route to chaos<sup>57</sup> and a period-doubling route to chaos<sup>58</sup> have been reported. Adding a fourth contact section for separated phase control in a longer (1 cm) passive waveguide has enabled achievement of a period-doubling route to chaos with much higher dimension<sup>59</sup>. In a recent proposal, the linear waveguide is replaced with an architecture based on a ring passive waveguide with a length of about 1 cm that integrates a DFB section, two semiconductor optical amplifier (SOA) sections and a photodiode (Fig. 2i). The larger feedback strength enables a dynamical regime of strong competition between  $f_{\text{RO}}$  and  $f_{\text{EC}}$  such that chaos is achieved with both high dimension and a featureless broadband power spectrum<sup>60</sup>.

Combining two DFB lasing sections separated by a passive waveguide leads to optical chaos in a tandem semiconductor laser<sup>61</sup> (Fig. 2h). The three contacts allow control of the frequency detuning, injection strength and phase shift of the mutually coupled lasers, hence accessing chaotic dynamics.

**Mode competition.** In some laser diodes that emit in several longitudinal, transverse or polarization modes, a sufficiently strong nonlinear mode coupling may induce chaotic instabilities even in the absence of additional parameter modulation, injection or feedback (Fig. 2j). For example, VCSELs typically emit in several polarization modes whose selection results from several mechanisms including a nonlinear coupling of circularly polarized field components through carrier spin-flip relaxation mechanisms<sup>62</sup>. This mechanism for VCSEL polarization selection is accompanied by a sequence of bifurcations to low-dimensional polarization chaos<sup>63</sup>. Also, broad-area semiconductor lasers may experience strong coupling between spatial transverse modes through carrier diffusion leading to a large variety of complex spatial patterns including wave chaos<sup>64</sup>.

**Nonlinear hybrid optoelectronic feedback.** In the previously described configurations, optical chaos is achieved from the nonlinear coupling between the lasing electric field and the carrier density. Another approach, inspired by the work of Ikeda on passive optical cavities with time-delayed feedback<sup>65</sup>, involves combining a laser diode with an optoelectronic feedback loop that contains a nonlinear optical device.

The so-called wavelength chaos generator uses a wavelength-tunable two-electrode distributed Bragg reflector (DBR) laser diode with a birefringent crystal placed between two crossed-polarizers<sup>66</sup> (Fig. 2k). This nonlinear optical device is used as an interferometer that converts a variation of the wavelength into a variation of the light intensity through a nonlinear function. The intensity change is then converted to an electrical current that is delayed and

amplified before driving the laser DBR section, hence impacting the wavelength dynamics. The physics underlying chaos is similar to the one resulting from the Ikeda equation for delayed passive Kerr cavities<sup>65</sup>.

Another way to modulate an optical interference function is to use a Mach-Zehnder modulator (Fig. 2l). The intensity of the light emitted by a continuous-wave 1.55 μm DFB laser is modulated using the Pockels electro-optic effect in a LiNbO<sub>3</sub> crystal in one arm of the interferometer. When the signals recombine at the output, the resulting interference depends on both the constant and fluctuating voltages applied to the two electrodes across the crystal. The feedback loop provides both low-pass and high-pass filtering described by a delayed integro-differential equation<sup>67</sup>. Both experiment and theory demonstrate a variety of new chaotic dynamics not observed in the conventional Ikeda equation. In particular, exploiting the form of the nonlinear interference function leads to chaotic dynamics with exceptionally flat power spectra over a large bandwidth<sup>68</sup>.

### Chaos communications

Several approaches have been adopted to perform digital communications using synchronized chaotic lasers<sup>69</sup>. Owing to their direct compatibility with existing optical fibre communications technology, semiconductor lasers have gained widespread attention for use in optical chaos communications.

**Chaos synchronization.** The fundamental requirement for performing communications using a chaotic carrier is achieving chaos synchronization. The work of Pecora and Carroll<sup>70</sup> stimulated the first observation of synchronization in lasers<sup>71</sup> and led to subsequent experimental realizations with, in particular, the first demonstration of chaos synchronization in external-cavity laser diodes<sup>72</sup>.

The generic experimental configuration (Fig. 3a) includes a transmitter or master laser and a receiver or slave laser. Unidirectional optical coupling between the transmitter and slave laser enables their synchronization. The transmitter laser is made chaotic using optical feedback from an external mirror—an external-cavity laser. The receiver laser may be configured as an external-cavity laser ('closed-loop') or else it may be a stand-alone laser whose dynamics is affected through optical coupling from the chaotic transmitter laser ('open-loop').

To clearly demonstrate the achievement of synchronization, a synchronization diagram is obtained (Fig. 3b). For two perfectly synchronized lasers, the synchronization diagram will be a straight line with a positive gradient. Adjustment of both the strength of the optical coupling and the frequency detuning between the two laser diodes has been shown to affect the synchronization between the lasers<sup>73,74</sup>. Mapping the synchronization quality in the plane of the coupling parameters unveils two regions of different synchronization properties<sup>75</sup> (Fig. 3c). For strong injection, synchronization occurs through nonlinear amplification of the slave laser and the corresponding parameter region is bounded by bifurcations delimiting injection-locking in the laser diode. Such synchronization is said to be 'generalized' as the receiver laser reproduces an amplified version of the transmitter output. At low injection strength, a much narrower synchronization region is found where the receiver emits a replica of the transmitter laser output ('identical' or 'complete' synchronization). Varying the detuning, a negative gradient was found in the synchronization diagram and termed inverse synchronization<sup>76</sup> or anti-synchronization<sup>77</sup>.

**Lag/lead/contemporaneous synchronization.** As observed numerically<sup>78</sup> and experimentally<sup>73</sup>, in generalized synchronization the slave laser output at a given time synchronizes with the master laser output taking account of a lag time arising from the time of flight between the lasers. In a state of complete synchronization, synchronization

occurs between the slave laser output and the time-shifted master laser output. The time-shift is determined by the difference between the coupling time and the external-cavity time-delay, as shown numerically<sup>79</sup> and experimentally<sup>80</sup>. Varying the time-delay, the slave laser output may therefore even anticipate that of the master laser<sup>80,81</sup>. Control of leader or laggard dynamics has been explored<sup>82</sup>, including demonstration of zero-lag long-range synchronization<sup>83</sup>.

**Message transmission.** The achievement of high-quality chaos synchronization enables message transmission using a chaotic carrier. The simple concept here is that a message added to a chaotic carrier generated in a transmitter laser can be recovered using a receiver laser in chaotic synchrony to the transmitter laser. Several schemes for message encoding have been explored and are summarized in Fig. 3d. They include (1) chaos masking, where the message is simply added to the chaotic carrier<sup>78</sup>; (2) chaos modulation—proposed for Chua's circuits<sup>84</sup> and used in the pioneering work on optical chaos communications by VanWiggeren and Roy<sup>85</sup>; (3) chaos shift keying (CSK)<sup>86</sup>, where digital ones and zeros are associated with distinct states; (4) on-off shift keying (OOSK)<sup>87</sup>, where the system is synchronized for say a one but is unsynchronized for a zero. The CSK scheme offers greater security but is more difficult to implement. In addition, the need to be able to identify the defined states adds a latency to the decoding process that will reduce the achievable bit-rate in transmission. A similar limitation arises for OOSK. To achieve high bit-rate chaotic optical communications, attention needs to be paid to the impact of noise that, in particular, may affect the quality of synchronization and even cause desynchronization<sup>88</sup>.

Using such encoding techniques, much effort has been directed to laboratory demonstrations of chaos communications using laser diodes. Such demonstrations included effecting network operations such as message relay<sup>89</sup> and message broadcasting<sup>90</sup>. An experimental arrangement for chaos broadcasting is illustrated in Fig. 3e. Good chaos synchronization is achieved between the transmitter and the first receiver (RL1) and between the transmitter and the second receiver (RL2).

However the most significant experimental achievement was a field trial that demonstrated that chaos communications could be effective over the 120 km metropolitan area network of Athens, Greece<sup>91</sup> (Fig. 3f). This was a key demonstration of the suitability of the approach for practical deployment over installed fibre-optic communication channels.

**Multiplexed chaotic communications.** A prominent feature of advanced optical communications systems is their capability to multiplex several laser wavelengths—through so-called wavelength division multiplexed (WDM) operation. To effect WDM operation it was shown that the longitudinal modes of two single-mode lasers may be chaos-synchronized to longitudinal modes of a multi-mode laser<sup>92</sup>. Similar multiplexed chaos synchronization was achieved between either transverse modes or polarization modes of VCSELs<sup>93</sup>. Selection of the polarization state of the coupled light in VCSELs allows synchronization of the polarization modes while keeping the total intensities desynchronized<sup>93</sup>.

However, these approaches to multiplexing chaotic light require as many lasers or modes as the number of users. A more spectrally efficient approach has been suggested. Multiplexed encryption using chaotic systems with multiple stochastic-delayed feedbacks has been used to experimentally demonstrate data transmission and recovery between multiple users at rates of several Gbits s<sup>-1</sup> on a single communication channel<sup>94</sup>. Alternatively, a specific coupling scheme was suggested where a pair of laser diodes synchronize to their counterpart at the receiver side although the transmitter lasers lase at the same wavelength and their outputs are combined in a single communication channel<sup>95</sup>.

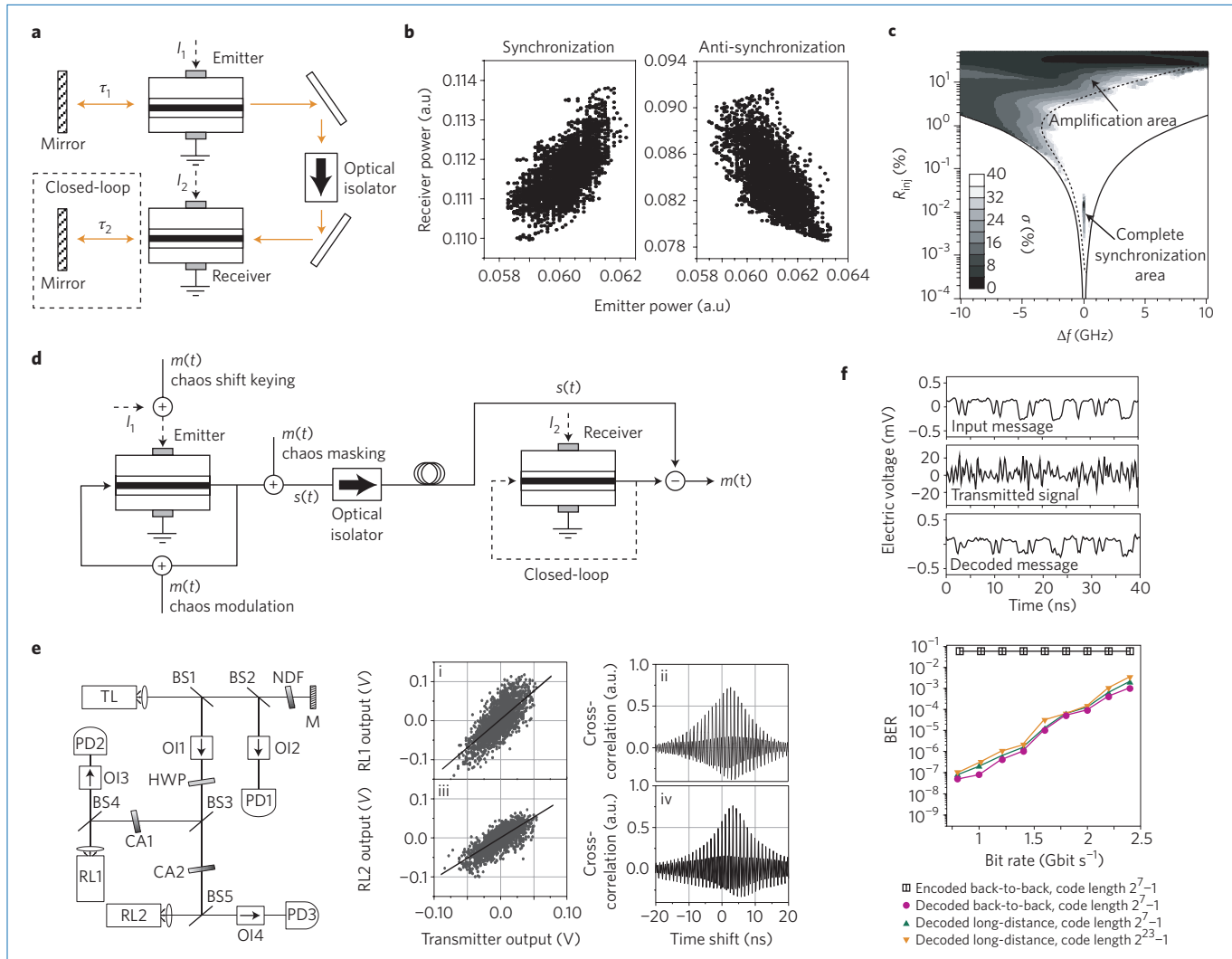


**Figure 3 | Chaos synchronization and chaos communication using laser diodes.** **a**, Schematic plot of a chaos synchronization experiment. An external-cavity laser diode (optical feedback from a mirror with a time-delay  $\tau_1$ ) synchronizes its chaotic dynamics with a receiver laser. If the receiver laser is also an external-cavity laser the configuration is termed 'closed loop'. **b**, Synchronization diagram showing the receiver output power versus the emitter output power. Perfect synchronization would mean a straight line in this diagram. Both synchronization and anti-synchronization have been observed. Reproduced from ref. 76, APS. **c**, Mapping of the synchronization quality in the plane of the injection parameters (injection strength  $R_{\text{inj}}$  versus frequency detuning  $\Delta f$ ). A grey scale is used to quantify the synchronization error,  $\sigma$ , with black representing no error and thus a high synchronization quality. Reproduced from ref. 75, APS. **d**, Schematic of the different possibilities for encoding a message,  $m(t)$ , into a chaotic carrier generated by a laser diode. In chaos masking the message is simply added to the laser output. In chaos modulation the message is added to the laser output but it also impacts the laser diode dynamics. In chaos shift keying the message is typically applied as a digital modulation of the driving current (or any of the laser parameters) such that two distinct chaotic dynamics are generated for bits 0 and 1 of the message. Following synchronization of the receiver, the message,  $m(t)$ , is extracted by subtracting the receiver output from the signal  $s(t)$  that is injected to the receiver laser. **e**, Experimental realization of message broadcasting using chaos synchronization of laser diodes. Panels i and iii show the synchronization plot of the two receivers, RL1 and RL2, with respect to the transmitter (TL), respectively. Panels ii and iv are the corresponding cross-correlation plots. PD, photodiode; CA, coupling attenuator; HWP, half-wave plate; BS, beam splitter; OI, optical isolator; NDF, neutral density filter; M, mirror. Reproduced from ref. 132, IET. **f**, First experimental realization of chaos communication on a fibre-optic network. The message is well decoded at the receiver side although it appears completely masked in the transmitted signal. The BER, however, increases with increasing bit rate due to degradation of the synchronization quality. Reproduced from ref. 91, NPG.

**Optimized communications and transmission security.** To enable effective chaos communications a minimal message strength is required to ensure acceptable bit error rates (BER) in transmission. However, the use of a very strong message may compromise the privacy of the message transmission. It is possible to identify optimized regimes of operation where those requirements are balanced<sup>96</sup>. The privacy of chaos communications rests on hardware keys and notably the device parameters of the transmitter and receiver lasers, which need to be rather closely matched to achieve high-quality synchronization. Although not guaranteed, security is greatly

enhanced by either arranging that synchronization is only possible for a narrow range of parameters, or with a chaotic transmitter of high enough complexity to prevent reconstruction from time-series analysis. In this respect, one would favor schemes that make the synchronization extremely sensitive to parameters (for example, closed loop configuration) or dependent on many degrees of freedom (such as in coupled VCSELs with polarization-dependent injection<sup>93</sup>). Reconstruction of the chaotic attractor from the observed system output requires the identification of the system parameters. For external-cavity lasers the time-delay in the external cavity and

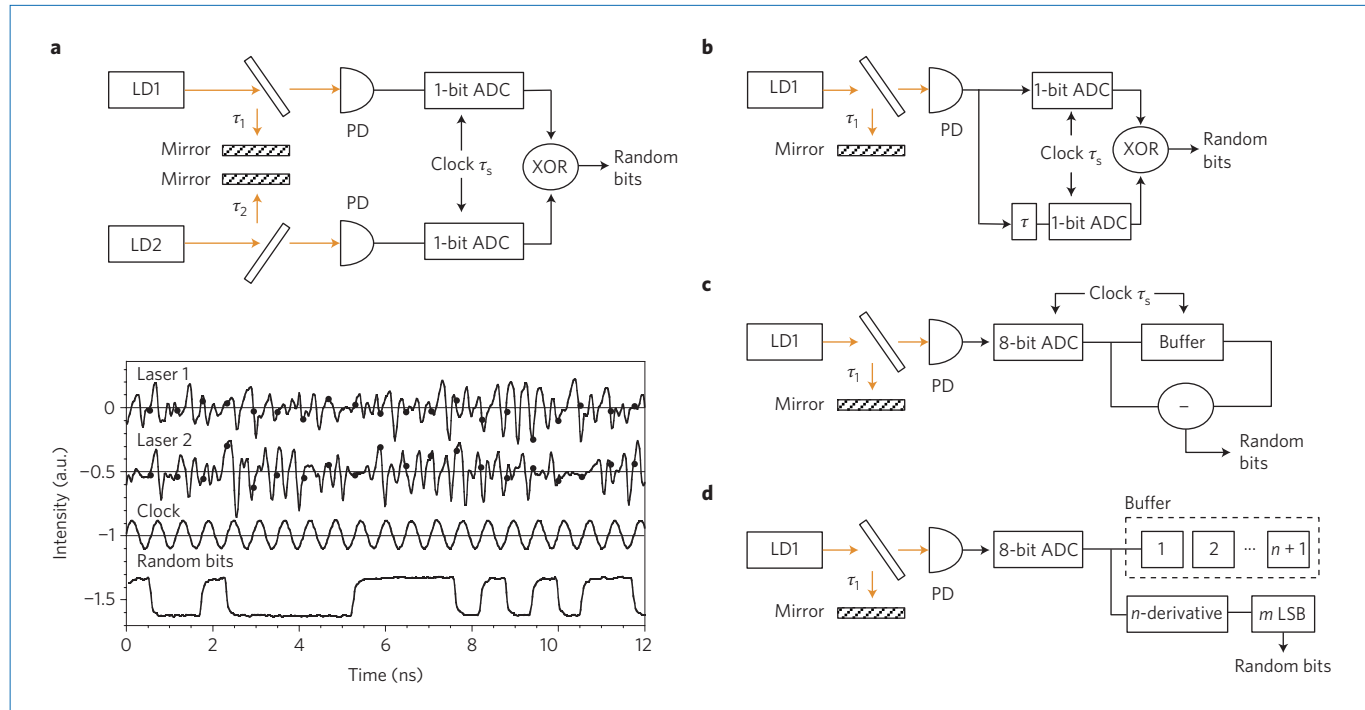


**Figure 4 | Random number generation (RNG) using chaos from a laser diode.** **a**, Schematic of the first experimental realization using two external-cavity laser diodes (LD1 and LD2) and a XOR logical operation applied to their 1-bit digitized outputs. ADC, analog-to-digital converter. The clock sampling time,  $\tau_s$ , and the two external-cavity delay times,  $\tau_1$  and  $\tau_2$ , must be incommensurate to avoid recurrences in the random bits. The bottom panel shows the experimental result with the generation of a random bit sequence at a bit rate of  $1.7 \text{ Gb s}^{-1}$ . Reproduced from ref. 106, NPG. **b-d**, Different realizations of the post-processing that improve the produced random bit rate.

the optical feedback strengths are key parameters in determining the laser dynamics. It has been shown that it is possible to extract the time-delay from the laser dynamics<sup>97</sup> and hence measures are required to counteract such a potential breach of security. Several means for concealing the time-delay value are available: setting the time-delay close to the time-period of the relaxation oscillations<sup>98</sup>, using more than one time-delayed feedback<sup>99</sup>, using stochastically varying or modulated time-delay values in the feedback loop<sup>94</sup>, or exploiting the polarization properties of VCSELs<sup>99</sup>. Optimization of chaos communication parameters also benefits from recent investigations of complexity measures from experimental time-series<sup>100–102</sup>. Besides conventional algorithms that compute Lyapunov exponents, recent approaches using permutation entropy have shown a greater robustness of the complexity analysis against the noise that is inevitably present in experimental chaotic time-series<sup>103</sup>. Detailed mappings of the laser diode dynamics with optical feedback based on permutation entropy have identified those parameter regions where high complexity (a large permutation entropy value) and a weak signature of laser parameters in the chaotic dynamics (in particular time-delay concealment) can be achieved simultaneously<sup>102</sup>.

### Random number generation

Although by nature distinct, chaos and randomness share a common feature in that they produce entropy. The Kolmogorov–Sinai entropy,  $K$ , is estimated from the sum of all positive Lyapunov exponents,  $\sum_i \lambda_i$ , and quantifies the sensitivity of chaos to initial conditions. The Shannon entropy,  $H(X) = \sum_i P(x_i) \log_2 P(x_i)$ , measures the information content arising from uncertainty of the random variable  $X$ , where  $P(x_i)$  is the probability of the value  $x_i$ . For example, a fair coin toss has one bit of Shannon entropy because there are two possible outcomes (head or tail) that occur with equal probability. As commonly observed, any microscopic noise inevitably present in a chaotic system acts to amplify the divergence of nearby system

trajectories in phase space. As time passes, the chaotic dynamics yields a Shannon information theoretic entropy directly related to the rate of growth of the divergence of system trajectories, that is, to the Kolmogorov–Sinai entropy. Digitizing the chaotic output on one bit, the chaotic dynamics can ideally produce up to the maximum one bit of entropy as in fair coin tossing but at a rate up to the magnitude of the Lyapunov exponent.

Laser diode-based chaos therefore provides an ideal physical source of random bits, as it combines outcome-unpredictability with no dependence on any previous outcome—two commonly accepted requirements for random number generation<sup>104</sup>. Also, chaotic laser diodes may produce a large number of positive Lyapunov exponents, whose magnitudes relate to laser frequencies that can be made very large. Random bits can therefore be produced at a much higher rate than other physical sources of entropy including quantum random number generators<sup>105</sup>.

Since its first demonstration in 2008<sup>106</sup>, the field of random number generation (RNG) using chaotic laser diodes has benefited from several developments. In the initial scheme (Fig. 4a), a chaotic external-cavity laser diode was used. The feedback strength and the injection current are adjusted giving chaotic dynamics with a flat power spectrum with a bandwidth of about 10 GHz. A 1-bit analog-to-digital converter (ADC) was used to produce the sequence of bits. However, sampling the chaotic output of a single laser diode did not produce an equal distribution of zeros and ones, that is, this would not make a fair coin, hence limiting the entropy. A second chaotic laser diode of the same type with its digitized output combined with the first using an XOR logical operation was then used. By making the time-delays of both external cavities and the sampling time of the ADC incommensurate, a  $1.7 \text{ Gb s}^{-1}$  sequence of bits that passed randomness statistical tests was achieved. Shortly afterwards, this scheme was simplified using only one chaotic laser diode and comparing its digitized output with a time-shifted version of it<sup>107</sup> (Fig. 4b). Again, the time-shift,

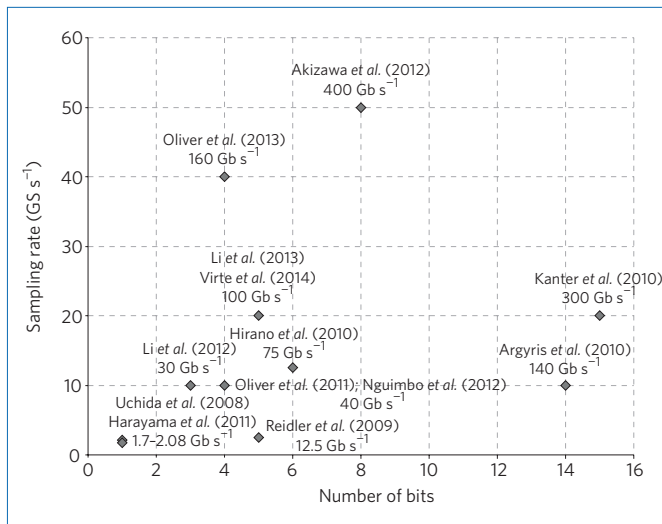


**Figure 5 | The state-of-the-art of random number generation using chaos from a laser diode.** Realizations differ by either the system under investigation, the post-processing method, the number of bits and/or the sampling rate. Each point corresponds one row, or multiple rows, in Table 1.

time-delay of the external-cavity and sampling clock time must be incommensurate to avoid any recurrence in the output.

Following that initial demonstration, several schemes were developed to improve the RNG performance, either focusing on the post-processing or on the physics of the laser diode chaos. The state-of-the-art is summarized in Fig. 5 and Table 1.

Instead of using a 1-bit ADC, benefit was derived from the use of multi-bit extraction<sup>108</sup>. Keeping the  $m$  least significant bits (LSBs) of the comparison between the digitized chaotic laser output and a time-shifted version (Fig. 4c), RNG at a rate of 12.5  $\text{Gb s}^{-1}$  was demonstrated. The generation rate has naturally increased by considering more bits but also because the multi-bit extraction improves the symmetry of the distribution of zeros and ones, hence removing the inherent bias in the outcome. Instead of a single comparison (first order derivative) the same research group suggested the use of high-order derivatives<sup>109</sup>. Keeping  $m$  LSBs of the  $n$ th order derivative (Fig. 4d) results in generation rates of up to 300  $\text{Gb s}^{-1}$  because the post-processing provides additional bits and improves the entropy growth rate, hence allowing for a higher sampling rate.

Experiments have suggested that the performance of optical chaos-based RNG increases with improved flatness and bandwidth of the generated chaos<sup>110</sup>. Among the well-known techniques for bandwidth enhancement, using optical injection allows the spectral translation of the chaotic bandwidth of a master laser towards the relaxation oscillation frequency of the injected slave laser. Increasing the chaos bandwidth up to about 16.5 GHz (ref. 107) has enabled the use of a 12.5  $\text{Gb s}^{-1}$  sampling rate on the six-LSB output of the digitized chaos, that is, 75  $\text{Gb s}^{-1}$  RNG. The same set-up but using reverse bit order sequence in the time-shifted laser output before applying the XOR logical operation uses the full 8-bit ADC resolution at the maximum sampling rate (50  $\text{Gb s}^{-1}$ ), hence achieving the current record rate of 400  $\text{Gb s}^{-1}$  (ref. 111).

Inspired by previous work using chaotic laser diodes employing external optical feedback, numerous works have shown good RNG performance using integrated chaotic laser diodes. The same set-up as the one used in 2008<sup>106</sup> has been employed with DFB lasers integrated within a 1-cm-long passive cavity<sup>112</sup>. The resulting flat power spectrum provides 2.08  $\text{Gb s}^{-1}$  RNG using single-bit extraction. A similar performance (1.56  $\text{Gb s}^{-1}$ ) has been achieved using a ring passive waveguide implementing optical feedback on a DFB laser with two SOA gain sections<sup>60</sup>. The use of multi-bit extraction with an integrated DFB laser with a 1 cm passive waveguide has been suggested to use 14 LSBs out of a 16-bit-ADC at a sampling rate of 10  $\text{Gb s}^{-1}$ , hence increasing the bit rate to 140  $\text{Gb s}^{-1}$  (ref. 113).

Although optical feedback is an efficient technique for obtaining high-bandwidth chaos with a large set of positive Lyapunov exponents, the time-delay periodicity imprinted in the laser output leads to recurrences in the outcome and the set-up requires a fine-tuning of the external cavity. A recent alternative was demonstrated using polarization chaos from a free-running VCSEL<sup>114</sup>: the 5 LSBs of the 8-bit-digitized polarized light output are used at a sampling rate of 20  $\text{Gb s}^{-1}$ , hence producing 100  $\text{Gb s}^{-1}$  physical RNG, successfully passing standard statistical tests for randomness. Promising results (up to 30  $\text{Gb s}^{-1}$  RNG) have also been obtained using the oversampling of 1.5 GHz low-pass filtered chaotic dynamics achieved by optical injection into a DFB laser diode<sup>115</sup>.

### Chaotic optical sensing

Chaotic lasers also have applications in high-precision ranging—so-called noise radar or correlation radar<sup>116</sup>, also known as chaotic radar<sup>117</sup> (CRADAR). The use of chaotic pulse trains in correlation radar offers a high-bandwidth to enable high-precision range measurements. Rapid decorrelation due to irregular pulse

**Table 1 | State-of-the-art random number generation using laser diode chaos.**

Year	System	Post-processing	Bits	Sampling rate ( $\text{GS s}^{-1}$ )	Bit rate ( $\text{Gb s}^{-1}$ )	Reference
2008	(LD+OF) $\times 2$	XOR	1	1.7	1.7	Uchida et al. 2008, ref. 106
2009	LD+OF	8-bit + derivative + LSB	5	2.5	12.5	Reidler et al. 2009, ref. 108
2010	LD+OF	8-bit + nth derivative + LSB	15	20	300	Kanter et al. 2010, ref. 109
2010	(LD+OF) + (LD+OI)	8-bit + XOR + LSB	6	12.5	75	Hirano et al. 2010, ref. 107
2010	LD+OF	16-bit + LSB	14	10	140	Argyris et al. 2010, ref. 113
2011	(LD+OF) $\times 2$	XOR	1	2.08	2.08	Harayama et al. 2011, ref. 112
2011	LD + OF (polarization)	8-bit + LSB	4	10	40	Oliver et al. 2011, ref. 134
2012	(LD+OF) + (LD+OI)	8-bit + bit reverse + XOR	8	50	400	Akizawa et al. 2012, ref. 111
2012	LD+OI	8-bit + time-shift + XOR + LSB	3	10	30	Li et al. 2012, ref. 115
2012	SRL + OF	8-bit x2 + XOR	4	10	40	Nguimdo et al. 2012, ref. 133
2013	LD + OF (polarization)	8-bit + LSB	4	40	160	Oliver et al. 2013, ref. 110
2013	LD + OI	8-bit + time-shift + XOR + LSB	5	20	100	Li et al. 2013, ref. 135
2014	VCSEL	8-bit + time-shift + LSB	5	20	100	Virté et al. 2014, ref. 114

LD, laser diode; OF, optical feedback; OI, optical injection; SRL, semiconductor ring laser; VCSEL, vertical-cavity surface-emitting laser; LSB, least significant bit.

intervals and amplitudes yields unambiguous range measurements; improved signal-to-noise ratios are gained from the available high average pulse repetition frequencies. A proof of concept CRADAR system<sup>117</sup> using an optically injected semiconductor laser as the source of chaos achieved a range resolution of 9 cm, limited by the detection bandwidth. Chaotic laser diodes have also been used to enhance resolution in optical time domain reflectometry (OTDR)<sup>118</sup>. OTDR is a key diagnostic tool for testing optical-fibre transmission systems, for example. The challenges in OTDR are to increase the measurement range, enhance signal-to-noise ratios and improve spatial resolution. Using lasers driven into chaos by feedback from an optical fibre ring, a spatial resolution of 6 cm was achieved for distances in a range of 140 m (ref. 118). Again, resolution was limited by the bandwidth of the detection.

### Optical logic and chaos computing

Chaos has also been proposed as a novel means for performing computing<sup>119</sup> and to implement optical logic functions<sup>120</sup>. A practical implementation of a NOR logic gate has been initially realized by applying a threshold function to the double-scroll chaotic attractor achieved in a Chua electronic circuit<sup>120</sup>. This proof-of-principle experiment demonstrates the universal computing capability of chaotic systems considering that all logic operations (AND, OR, NOT, XOR and NAND) can be constructed from combinations of NOR logic functions. Optoelectronic devices have been used to implement such logic elements<sup>121</sup>, including the use of chaotic two-section semiconductor lasers<sup>122</sup>. NOR logic operation is theoretically demonstrated by analysing the synchronization properties of two mutually coupled chaotic two-section laser diodes with initially identical laser parameters. By modulating the injection currents in both the gain and absorber sections of one of the two laser diodes (similar to what we defined previously as CSK), one achieves a situation where synchronization quality is high (output equal to one) only when the gain and absorber bias currents of both lasers are almost identical (when both modulated current inputs are zero). However, the processing speed of the resulting NOR gate is limited by the time for synchronization or desynchronization, which is typically around several nanoseconds.

### Outlook

To assess how this area of activity may evolve in the future it is appropriate to first reflect on the remarkable progress that has already been made. It is worth recalling some early scepticism among some members of the semiconductor laser community who considered that the complex dynamics of semiconductor lasers was just a hindrance to practical applications and so should be engineered out of existence. However, as appreciation grew for the universality of many nonlinear dynamical and chaotic phenomena, it became apparent that the laser diode provided an ideal testbed for investigations of novel dynamical behaviour. This attracted mathematicians and theoretical physicists who added to the insights and the armoury of techniques that could be used to explore laser diode dynamics. The richness of the dynamics that may be conveniently accessed in a variety of laser diode configurations augurs well that the field will remain a fertile area for exploration and exploitation for many years to come.

Exciting developments may be envisaged due to the continuing evolution of laser diode designs with particular opportunities arising with the demonstration of electrically pumped nanolasers<sup>123</sup>. Such nanolaser designs may incorporate plasmonic and spintronic features that will impact on the laser dynamics. Nanolasers are being developed for applications in such diverse fields as quantum computing and systems-on-a-chip. Much attention has been given in recent years to developing semiconductor lasers operating in the mid-infrared and terahertz regions of the electromagnetic spectrum. The quantum cascade laser (QCL), whose operation

relies on unipolar intersubband electronic transitions, is the most prominent semiconductor laser operating in this wavelength range. Because of the technological challenges that have needed to be surmounted to create viable QCLs, experimental investigation of their dynamical properties has been relatively limited, but nevertheless exploration of nonlinear dynamical properties has begun<sup>124</sup>. As the operability of QCLs develops, opportunities for exploiting their novel dynamical features will be created. Apart from working with existing semiconductor lasers, it is suggested that a fertile direction for development is the design of novel semiconductor lasers to exploit specific nonlinear dynamical phenomena. This cuts across the grain of much electronic engineering, where operation in the linear regime is preferred but with the available wide range of nonlinear dynamical phenomena one can expect that useful applications can be satisfied by deliberately emphasizing such aspects.

In terms of the engineering applications of laser diode chaos, a specific early focus was private optical communications. In particular, much effort was made within Europe to advance this technology. Although some of the momentum from that effort has been lost in recent years, there is evidence of continued interest in this topic elsewhere in the world, and notably in China. Given the changes that are occurring in the global economy it may be the case that deployment of secure chaos-based communications systems will come to fruition driven by the requirements of the growing Chinese economy.

Due to their ease of operation, laser diodes may be used to build experimental analogues of processes occurring in other fields. Thus, for example, time-delay effects in semiconductor lasers enable insights to be gained into synaptic behaviour in neurons<sup>125</sup>. As latency is a feature of many biological and physical systems, it is expected that such analogies can be profitably used in many other cases. In some parameter ranges, laser diode dynamics with optical injection<sup>126</sup> or optical feedback<sup>127</sup> show similar extreme event statistics as those characterizing rogue waves in hydrodynamics<sup>128</sup>. The statistical analysis used here takes advantage of the frequencies of the processes involved being much higher than in fluid dynamics. Another example is found in the study of dissipative systems. Many of the features of spatial dissipative solitons including chaotic motions and the clustering of localized states<sup>129</sup> would benefit from the knowledge of coupled-laser chaotic oscillators.

It is suggested that a particular legacy of the wide-ranging explorations of laser diode chaos is an enhanced awareness of powerful techniques for characterizing and controlling complex dynamics. There is clear scope for wider application of such techniques. Currently, global attention is being given to the development of low-carbon economies. Photonics in general, and the laser diode in particular, has a direct role to play in that agenda with, for example, reducing energy consumption in optical communication networks<sup>130</sup> and efficient solid state lighting being key elements in the reduction of electricity consumption worldwide. However, an indirect impact can also be identified. The increased use of localized sustainable sources of electricity will create challenges in the control of complex distribution networks where nonlinear dynamical behaviour will arise. Insights derived from the exploration of nonlinear and chaotic dynamics in laser diode systems may be directly applicable to tackling such engineering challenges.

Received 26 June 2014; accepted 22 December 2014; published online 27 February 2015

### References

1. Maiman, T. H., Hoskins, R. H., D'Haenens, I. J., Asawa, C. K. & Evtuhov, V. Stimulated optical emission in fluorescent solids. II. Spectroscopy and stimulated emission in ruby. *Phys. Rev.* **123**, 1151–1157 (1961).
2. Kimura, T. & Otsuka, K. Response of a CW Nd<sup>3+</sup>:YAG laser to sinusoidal cavity perturbations. *IEEE J. Quantum Electron.* **6**, 764–769 (1970).

3. Lorenz, E. N. Deterministic non-periodic flow. *J. Atmos. Sci.* **20**, 130–141 (1963).
4. Mandelbrot, B. How long is the coast of Britain? Statistical self-similarity and fractional dimension. *Science* **156**, 636–638 (1967).
5. Li, T. Y. & Yorke, J. A. Period-three implies chaos. *Am. Math. Mon.* **82**, 985 (1975).
6. Wolf, A., Swift, J. B., Swinney, H. L. & Vastano, J. A. Determining Lyapunov exponents from a time-series. *Physica D* **16**, 285–317 (1985).
7. Grassberger, P. & Procaccia, I. Characterization of strange attractors. *Phys. Rev. Lett.* **50**, 346–349 (1983).
8. Haken, H. Analogies between higher instabilities in fluids and lasers. *Phys. Lett. A* **53**, 77–78 (1975).
9. Feigenbaum, M. J. The onset spectrum of turbulence. *Phys. Lett. A* **74**, 375–378 (1979).
10. Ruelle, D. & Takens, F. On the nature of turbulence. *Commun. Math. Phys.* **20**, 167–192 (1979).
11. Pomeau, Y. & Manneville, P. Intermittent transition to turbulence in dissipative dynamical systems. *Commun. Math. Phys.* **74**, 189–197 (1980).
12. Arechi, F. T., Meucci, R., Puccioni, G. P. & Tredicce, J. R. Experimental evidence of subharmonic bifurcations, multistability, and turbulence in a Q-switched gas laser. *Phys. Rev. Lett.* **49**, 1217–1220 (1982).
13. Midavaine, T., Dangoisse, D. & Glorieux, P. Observation of chaos in a frequency-modulated CO<sub>2</sub> laser. *Phys. Rev. Lett.* **55**, 1989–1992 (1985).
14. Weiss, C. O., Abraham, N. B. & Hubner, U. Homoclinic and heteroclinic chaos in a single-mode laser. *Phys. Rev. Lett.* **61**, 1587–1590 (1988).
15. Keller, U. Recent developments in compact ultrafast lasers. *Nature* **424**, 831–838 (2003).
16. Tredicce, J. R., Arechi, F. T., Lippi, G. L. & Puccioni, G. P. Instabilities in lasers with an injected signal. *J. Opt. Soc. Am. B* **2**, 173–183 (1985).
17. Henry, C. H. Theory of the linewidth of semiconductor lasers. *IEEE J. Quantum Electron.* **18**, 259–264 (1982).
18. Ohtsubo, J. *Semiconductor Lasers: Stability, Instability and Chaos* 3rd edn (Springer, 2013).
19. Luedge, K. *Nonlinear Laser Dynamics: From Quantum Dots to Cryptography* (Wiley-VCH, 2011).
20. Mukai, T. & Otsuka, K. New route to optical chaos: successive-subharmonic-oscillation cascade in a semiconductor laser coupled to an external cavity. *Phys. Rev. Lett.* **55**, 1711–1714 (1985).
21. Mork, J., Mark, J. & Tromborg, B. Route to chaos and competition between relaxation oscillations for a semiconductor laser with optical feedback. *Phys. Rev. Lett.* **65**, 1999–2002 (1990).
22. Erneux, T., Gavrielides, A. & Sciamanna, M. Stable microwave oscillations due to external-cavity-mode beating in laser diodes subject to optical feedback. *Phys. Rev. A* **66**, 033809 (2002).
23. Morikawa, T., Mitsuhashi, Y., Shimada, J. & Kojima, Y. Return-beam-induced oscillations in self-coupled semiconductor lasers. *Electron. Lett.* **12**, 435–436 (1976).
24. Lenstra, D., Verbeek, B. & Den Boef, A. Coherence collapse in single-mode semiconductor-lasers due to optical feedback. *IEEE J. Quantum Electron.* **21**, 674–679 (1985).
25. Vicente, R., Dauden, J., Colet, P. & Toral, R. Analysis and characterization of the hyperchaos generated by a semiconductor laser subject to a delayed feedback loop. *IEEE J. Quantum Electron.* **41**, 541–548 (2005).
26. Heil, T., Fischer, I., Elsaesser, W. & Gavrielides, A. Dynamics of semiconductor lasers subject to delayed optical feedback: the short cavity regime. *Phys. Rev. Lett.* **87**, 243901 (2001).
27. Murakami, A. & Ohtsubo, J. Dynamics of semiconductor lasers with optical feedback from photorefractive phase conjugate mirror. *Opt. Rev.* **6**, 359–364 (1999).
28. Karsaklian dal Bosco, A., Wolfersberger, D. & Sciamanna, M. Super-harmonic self-pulsations from a time-delayed phase-conjugate optical system. *Appl. Phys. Lett.* **105**, 081101 (2014).
29. Fischer, A. P. A., Yousefi, M., Lenstra, D., Carter, M. W. & Vemuri, G. Filtered optical feedback induced frequency dynamics in semiconductor lasers. *Phys. Rev. Lett.* **92**, 023901 (2004).
30. Giudici, M., Giuggioli, L., Green, C. & Tredicce, J. Dynamical behavior of semiconductor lasers with frequency selective optical feedback. *Chaos Soliton. Fract.* **10**, 811–818 (1999).
31. Hong, Y., Paul, J., Spencer, P. S. & Shore, K. A. The effects of polarization-resolved optical feedback on the relative intensity noise and polarization stability of vertical-cavity surface-emitting lasers. *IEEE J. Lightw. Technol.* **24**, 3210–3216 (2006).
32. Li, H., Hohl, A., Gavrielides, A., Hou, H. & Choquette, K. D. Stable polarization self-modulation in vertical-cavity surface-emitting lasers. *Appl. Phys. Lett.* **72**, 2355–2357 (1998).
33. Sciamanna, M. *et al.* Optical feedback induces polarization mode hopping in vertical-cavity surface-emitting lasers. *Opt. Lett.* **28**, 1543–1545 (2003).
34. Kane, D. M. & Shore, K. A. *Unlocking Dynamical Diversity: Optical Feedback Effects on Semiconductor Lasers* (Wiley, 2005).
35. Soriano, M. C., Garcia-Ojalvo, J., Mirasso, C. R. & Fischer, I. Complex photonics: dynamics and applications of delay-coupled semiconductor lasers. *Rev. Mod. Phys.* **85**, 421–470 (2013).
36. Simpson, T. B., Liu, J. M., Gavrielides, A., Kovanic, V. & Alsing, P. M. Period-doubling route to chaos in a semiconductor laser subject to optical injection. *Appl. Phys. Lett.* **64**, 3539–3541 (1994).
37. Wieczorek, S., Krauskopf, B., Simpson, T. B. & Lenstra, D. The dynamical complexity of optically injected semiconductor lasers. *Phys. Rep.* **416**, 1–128 (2005).
38. Qi, X.-Q. & Liu, J. M. Photonic microwave applications of the dynamics of semiconductor lasers. *IEEE J. Sel. Topics Quantum Electron.* **17**, 1198–1211 (2011).
39. Chow, W. W. & Wieczorek, S. Using chaos for remote sensing of laser radiation. *Opt. Express* **17**, 7491–7504 (2009).
40. Gatare, I., Sciamanna, M., Buesa, J., Thienpont, H. & Panajotov, K. Nonlinear dynamics accompanying polarization switching in vertical-cavity surface-emitting lasers with orthogonal optical injection. *Appl. Phys. Lett.* **88**, 101106 (2006).
41. Wu, D. S., Slavik, R., Marra, G. & Richardson, D. J. Direct selection and amplification of individual narrowly spaced optical comb modes via injection locking: design and characterization. *IEEE J. Lightw. Technol.* **31**, 2287–2295 (2013).
42. Lee, C. H., Yoon, T.-H. & Shin, S.-Y. Period doubling and chaos in a directly modulated laser diode. *Appl. Phys. Lett.* **46**, 95–97 (1985).
43. Chen, Y. C., Winful, H. G. & Liu, J. M. Subharmonic bifurcations and irregular pulsing behavior of modulated semiconductor lasers. *Appl. Phys. Lett.* **47**, 208–210 (1985).
44. Liu, H.-F. & Ngai, W. F. Nonlinear dynamics of a directly modulated 1.55 μm InGaAsP distributed feedback semiconductor laser. *IEEE J. Quantum Electron.* **29**, 1668–1675 (1993).
45. Sciamanna, M., Valle, A., Mégret, P., Blondel, M. & Panajotov, K. Nonlinear polarization dynamics in directly modulated vertical-cavity surface-emitting lasers. *Phys. Rev. E* **68**, 016207 (2003).
46. Vladimirov, A. G., Pimenov, A. S. & Rachinskii, D. Numerical study of dynamical regimes in a monolithic passively mode-locked semiconductor laser. *IEEE J. Quantum Electron.* **45**, 462–468 (2009).
47. Bandelow, U., Radzunias, M., Vladimirov A. G., Hüttl, B. & Kaiser, R. 40 GHz mode-locked semiconductor lasers: theory, simulations and experiment. *Opt. Quantum Electron.* **38**, 495–512 (2006).
48. Viktorov, E. A. *et al.* Stability of the mode-locked regime in quantum dot lasers. *Appl. Phys. Lett.* **91**, 231116–231118 (2007).
49. Duan, G. H. & Landais, P. Self-pulsation in multielectrode distributed feedback lasers. *IEEE Photon. Technol. Lett.* **7**, 278–280 (1995).
50. Mesaritakis, Ch. *et al.* Chaotic emission and tunable self-sustained pulsations in a two-section Fabry–Perot quantum dot laser. *Appl. Phys. Lett.* **98**, 051104 (2011).
51. Yamada, M. A theoretical analysis of self-sustained pulsation phenomena in narrow-stripe semiconductor lasers. *IEEE J. Quantum Electron.* **29**, 1330 (1993).
52. Kawaguchi, H. A theoretical analysis of self-sustained pulsation phenomena in narrow-stripe semiconductor lasers. *Appl. Phys. Lett.* **45**, 1264 (1984).
53. Yamada, M. *et al.* Experimental characterization of the feedback induced noise in self-pulsing lasers. *IEICE T. Electron.* **E82-C**, 2241–2247 (1999).
54. Tang, S. & Liu, J. M. Chaotic pulsing and quasi-periodic route to chaos in a semiconductor laser with delayed opto-electronic feedback. *IEEE J. Quantum Electron.* **37**, 329–336 (2001).
55. Lin, F.-Y. & Liu, J. M. Nonlinear dynamics of a semiconductor laser with delayed negative optoelectronic feedback. *IEEE J. Quantum Electron.* **39**, 562–568 (2003).
56. Bauer, S. *et al.* Nonlinear dynamics of semiconductor lasers with active optical feedback. *Phys. Rev. E* **69**, 016206 (2004).
57. Uchakov, O. V., Korneyev, N., Radzunias, M., Wünsche, H.-J. & Henneberger, F. Excitability of chaotic transients in a semiconductor laser. *Europhys. Lett.* **79**, 30004 (2007).
58. Wu, J.-G. *et al.* Direct generation of broadband chaos by a monolithic integrated semiconductor laser chip. *Opt. Express* **21**, 23358–23364 (2013).
59. Argyris, A., Hamacher, M., Chlouverakis, K. E., Bogris, A. & Syvridis, D. Photonic integrated device for chaos applications in communications. *Phys. Rev. Lett.* **100**, 194101 (2008).
60. Sunada, S. *et al.* Chaos laser chips with delayed optical feedback using a passive ring waveguide. *Opt. Express* **19**, 5713–5724 (2011).
61. Shikora, S., Wünsche, H.-J. & Henneberger, F. All-optical noninvasive chaos control of a semiconductor laser. *Phys. Rev. E* **78**, 025202(R) (2008).
62. San Miguel, M., Feng, Q. & Moloney, J. V. Light-polarization dynamics in surface-emitting semiconductor lasers. *Phys. Rev. A* **52**, 1728 (1995).

63. Virte, M., Panajotov, K., Thienpont, H. & Sciamanna, M. Deterministic polarization chaos from a laser diode. *Nature Photon.* **7**, 60–65 (2013).
64. Marciante, J. R. & Agrawal, G. P. Spatio-temporal characteristics of filamentation in broad-area semiconductor lasers: experimental results. *IEEE Photon. Technol. Lett.* **10**, 54–56 (1998).
65. Ikeda, K. Multiple-valued stationary state and its instability of the transmitted light by a ring cavity system. *Opt. Commun.* **30**, 257–261 (1979).
66. Goedgebuer, J. P., Larger, L., Porte, H. & Delorme, F. Chaos in wavelength with a feedback tunable laser diode. *Phys. Rev. E* **57**, 2795–2798 (1998).
67. Peil, M., Jacquot, M., Chembo, Y., Larger, L. & Erneux, T. Routes to chaos and multiple time scale dynamics in broadband bandpass nonlinear delay electro-optic oscillators. *Phys. Rev. E* **79**, 026208 (2009).
68. Callan, K. E., Illing, L., Gao, Z., Gauthier, D. J. & Schöll, E. Broadband chaos generated by an optoelectronic oscillator. *Phys. Rev. Lett.* **104**, 113901 (2010).
69. Colet, P. & Roy, R. Digital communication with synchronized chaotic lasers. *Opt. Lett.* **19**, 2056–2058 (1996).
70. Pecora, L. & Carroll, T. L. Synchronization in chaotic systems. *Phys. Rev. Lett.* **64**, 821–824 (1990).
71. Roy, R. & Thornburg, K. S. Jr Experimental synchronization of chaotic lasers. *Phys. Rev. Lett.* **72**, 2009–2012 (1994).
72. Sivaprakasam, S. & Shore, K. A. Demonstration of optical synchronization of chaotic external-cavity laser diodes. *Opt. Lett.* **24**, 466–468 (1999).
73. Sivaprakasam, S. & Shore, K. A. Message encoding and decoding using chaotic external-cavity diode lasers. *IEEE J. Quantum Electron.* **36**, 35–39 (2000).
74. Spencer, P. S. & Mirasso, C. R. Analysis of optical chaos synchronization in frequency-detuned external-cavity VCSELs. *IEEE J. Quantum Electron.* **35**, 803–808 (1999).
75. Murakami, A. & Ohtsubo, J. Synchronization of feedback-induced chaos in semiconductor lasers by optical injection. *Phys. Rev. A* **65**, 033826 (2002).
76. Sivaprakasam, S. *et al.* Inverse synchronization in semiconductor laser diodes. *Phys. Rev. A* **64**, 013805 (2001).
77. Wedekind, I. & Parlitz, U. Experimental observation of synchronization and anti-synchronization of chaotic low-frequency fluctuations in external-cavity semiconductor lasers. *Int. J. Bifurcat. Chaos* **11**, 1141–1147 (2001).
78. Mirasso, C. R., Colet, P. & Garcia Fernandez, P. Synchronization of chaotic semiconductor lasers: application to encoded communications. *IEEE Photon. Technol. Lett.* **8**, 299–301 (1996).
79. Ahlers, V., Parlitz, U. & Lauterborn, W. Hyperchaotic dynamics and synchronization of external-cavity semiconductor lasers. *Phys. Rev. E* **58**, 7208–7213 (1998).
80. Liu, Y. *et al.* Experimental observation of complete chaos synchronization in semiconductor lasers. *Appl. Phys. Lett.* **80**, 4306–4308 (2002).
81. Masoller, C. Anticipation in the synchronization of chaotic semiconductor lasers with optical feedback. *Phys. Rev. Lett.* **86**, 2782–2785 (2001).
82. Gonzalez, C. M., Torrent, M. C. & Garcia-Ojalvo, J. M. Controlling the leader laggard dynamics in delay-synchronized lasers. *Chaos* **17**, 033122 (2007).
83. Fischer, I. *et al.* Zero lag long range synchronization via dynamical relaying. *Phys. Rev. Lett.* **97**, 123902 (2006).
84. Halle, K. S., Wu, C. W., Itoh, M. & Chua, L. O. Spread spectrum communication through modulation of chaos. *Int. J. Bifurcat. Chaos* **3**, 469–477 (1993).
85. VanWiggeren, G. D. & Roy, R. Communication with chaotic lasers. *Science* **279**, 1198–1200 (1998).
86. Parlitz, U., Chua, L. O., Kocarev, L., Halle, K. S. & Shang, A. Transmission of digital signals by chaotic synchronization. *Int. J. Bifurcat. Chaos* **2**, 973–977 (1992).
87. Heil, T. *et al.* ON/OFF phase shift keying for chaos-encrypted communication using external-cavity semiconductor lasers. *IEEE J. Quantum Electron.* **38**, 1162–1170 (2002).
88. Liu, J.-M., Chen, H.-F. & Tang, S. Synchronized chaotic optical communications at high bit rates. *IEEE J. Quantum Electron.* **38**, 1184–1196 (2002).
89. Lee, M. W. & Shore, K. A. Demonstration of a chaotic optical message relay using DFB laser diodes. *IEEE Photon. Technol. Lett.* **18**, 169–171 (2006).
90. Lee, M. W. & Shore, K. A. Chaotic message broadcasting using DFB laser diodes. *Electron. Lett.* **40**, 614–615 (2004).
91. Argyris, A. *et al.* Chaos-based communications at high bit rates using commercial fibre-optic links. *Nature* **438**, 343–346 (2005).
92. Lee, M. W. & Shore, K. A. Two-mode chaos synchronization using a multimode external-cavity laser diode and two single-mode laser diodes. *IEEE J. Lightw. Technol.* **23**, 1068–1073 (2005).
93. Sciamanna, M., Gatare, I., Locquet, A. & Panajotov, K. Polarization synchronization in unidirectionally coupled vertical-cavity surface-emitting lasers with orthogonal optical injection. *Phys. Rev. E* **75**, 056213 (2007).
94. Rontani, D., Sciamanna, M., Locquet, A. & Citrin, D. S. Multiplexed encryption using chaotic systems with multiple stochastic-delayed feedbacks. *Phys. Rev. E* **80**, 066209 (2009).
95. Rontani, D., Locquet, A., Sciamanna, M. & Citrin, D. S. Spectrally efficient multiplexing of chaotic light. *Opt. Lett.* **35**, 2016–2018 (2010).
96. Priyadarshi, S., Pierce, I., Hong, Y. & Shore, K. A. Optimal operating conditions for external cavity semiconductor laser optical chaos communication system. *Semicond. Sci. Tech.* **27**, 094002 (2012).
97. Büunner, M. J., Kittel, A., Parisi, J., Fischer, I. & Elsaesser, W. Estimation of delay times from a delayed optical feedback laser experiment. *Europhys. Lett.* **42**, 353 (1998).
98. Rontani, D., Locquet, A., Sciamanna, M. & Citrin, D. S. Loss of time-delay signature in the chaotic output of a semiconductor laser with optical feedback. *Opt. Lett.* **32**, 2960–2962 (2007).
99. Lin, H., Hong, Y. & Shore, K. A. Experimental study of time-delay signatures in vertical-cavity surface-emitting lasers subject to double-cavity polarization-rotated optical feedback. *IEEE J. Lightw. Technol.* **32**, 1829–1836 (2014).
100. Tiana-Alsina, J., Torrent, M. C., Rosso, O. A., Masoller, C. & Garcia-Ojalvo, J. Quantifying the statistical complexity of low-frequency fluctuations in semiconductor lasers with optical feedback. *Phys. Rev. A* **82**, 013819 (2010).
101. Zunino, L., Rosso, O. A. & Soriano, M. C. Characterizing the hyperchaotic dynamics of a semiconductor laser subject to optical feedback via permutation entropy. *IEEE J. Sel. Topics Quantum Electron.* **17**, 1250–1257 (2011).
102. Toomey, J. P. & Kane, D. M. Mapping the dynamic complexity of a semiconductor laser with optical feedback using permutation entropy. *Opt. Express* **22**, 1713–1725 (2014).
103. Bandt, Ch & Pompe, B. Permutation entropy: a natural complexity measure for time series. *Phys. Rev. Lett.* **88**, 174102 (2002).
104. Jennewein, T., Achleitner, U., Weihs, G., Weinfurter, H. & Zellinger, A. A fast and compact quantum random number generator. *Rev. Sci. Instrum.* **71**, 1675–1680 (2000).
105. Gabriel, C. *et al.* A generator for unique quantum random numbers based on vacuum states. *Nature Photon.* **4**, 711–715 (2010).
106. Uchida, A. *et al.* Fast physical random bit generation with chaotic semiconductor lasers. *Nature Photon.* **2**, 728–732 (2008).
107. Hirano, K. *et al.* Fast random bit generation with bandwidth-enhanced chaos in semiconductor lasers. *Opt. Express* **18**, 5512–5524 (2010).
108. Reidler, I., Aviad, Y., Rosenbluh, M. & Kanter, I. Ultrahigh-speed random number generation based on a chaotic semiconductor laser. *Phys. Rev. Lett.* **103**, 024102 (2009).
109. Kanter, I., Aviad, Y., Reidler, I., Cohen, E. & Rosenbluh, M. An optical ultrafast random bit generator. *Nature Photon.* **4**, 58–61 (2010).
110. Oliver, N., Soriano, M., Sukow, D. & Fischer, I. Fast random bit generation using a chaotic laser: approaching the information theoretic limit. *IEEE J. Quantum Electron.* **49**, 910–918 (2013).
111. Akizawa, T. *et al.* Fast random number generation with bandwidth-enhanced chaotic semiconductor lasers at 8 × 50 Gb/s. *IEEE Photon. Technol. Lett.* **24**, 1042–1044 (2012).
112. Hayama, T. *et al.* Fast nondeterministic random-bit generation using on-chip chaos lasers. *Phys. Rev. A* **83**, 031803(R) (2011).
113. Argyris, A., Degliannidis, S., Pikasis, E., Bogris, A. & Syvridis, D. Implementation of 140 Gb s<sup>-1</sup> true random bit generator based on a chaotic photonic integrated circuit. *Opt. Express* **18**, 18763–18768 (2010).
114. Virte, M., Mercier, E., Thienpont, H., Panajotov, K. & Sciamanna, M. Physical random bit generation from chaotic solitary laser diode. *Opt. Express* **22**, 17271–17280 (2014).
115. Li, X.-Z. & Chan, S.-C. Random bit generation using an optically injected semiconductor laser in chaos with oversampling. *Opt. Lett.* **37**, 2163–2165 (2012).
116. Myneni, K., Barr, T. A., Reed, B. R., Pethel, S. D. & Corron, N. J. High-precision ranging using a chaotic laser pulse train. *Appl. Phys. Lett.* **78**, 1496–1498 (2001).
117. Lin, F. Y. & Liu, J. M. Chaotic radar using nonlinear laser dynamics. *IEEE J. Quantum Electron.* **40**, 815–820 (2004).
118. Wang, Y., Wang, B. & Wang, A. Chaotic correlation optical time domain reflectometer utilizing laser diode. *IEEE Photon. Technol. Lett.* **20**, 1636–1638 (2008).
119. Sinha, S. & Ditto, W. L. Dynamics based computation. *Phys. Rev. Lett.* **81**, 2156–2159 (1998).
120. Murali, K., Sinha, S. & Ditto, W. L. Implementation of NOR gate by a chaotic Chua's circuit. *Int. J. Bifurcat. Chaos* **13**, 2669–2672 (2003).
121. Kim, J. Y., Kang, J. M., Kim, T. K. & Han, S. K. 10 Gbit s<sup>-1</sup> all-optical composite logic gates with XOR, NOR, OR and NAND functions using SOA-MZI structures. *Electron. Lett.* **42**, 303–304 (2006).
122. Chlouverakis, K. A. & Adams, M. J. Optoelectronic realisation of NOR logic gate using chaotic two-section lasers. *Electron. Lett.* **41**, 359–360 (2005).
123. Khurgin, J. B. & Sun, G. Comparative analysis of spasers, vertical-cavity surface-emitting lasers and surface-plasmon emitting diodes. *Nature Photon.* **8**, 468–473 (2014).

124. Wojcik, A. K., Yu, N., Diehl, L., Capasso, F. & Belyanin, A. Nonlinear dynamics of coupled transverse modes in quantum cascade lasers. *J. Mod. Opt.* **7**, 1892–1899 (2010).
125. Manju Shrii, M., Senthilkumar, D. V. & Kurths, J. Delay-induced synchrony in complex networks with conjugate coupling. *Phys. Rev. E* **85**, 057203 (2012).
126. Bonatto, C. *et al.* Deterministic optical rogue waves. *Phys. Rev. Lett.* **107**, 053901 (2011).
127. Karsaklian dal Bosco, A., Wolfersberger, D. & Sciamanna, M. Extreme events in time-delayed nonlinear optics. *Opt. Lett.* **38**, 703–705 (2013).
128. Dudley, J. M., Dias, F., Erkintalo, M. & Genty, G. Instabilities, breathers and rogue waves in optics. *Nature Photon.* **8**, 755–764 (2014).
129. Verschueren, N., Bortolozzo, U., Clerc, M. G. & Residori, S. Spatiotemporal chaotic localized state in liquid crystal light valve experiments with optical feedback. *Phys. Rev. Lett.* **110**, 104101 (2013).
130. Tucker, R. S. Green optical communications — part II: energy limitations in transport. *IEEE J. Sel. Topics Quantum Electron.* **17**, 245–260 (2011).
131. Hübner, U., Abraham, N. B. & Weiss, C. O. Dimensions and entropies of chaotic intensity pulsations in a single-mode far-infrared NH<sub>3</sub> laser. *Phys. Rev. A* **40**, 6354–6365 (1989).
132. Lee, M. W. & Shore, K. A. Chaotic message broadcasting using DFB laser diodes. *Electron. Lett.* **40**, 614–615 (2004).
133. Nguimdo, R. M. *et al.* Fast random bits generation based on a single chaotic semiconductor ring laser. *Opt. Express* **20**, 28603–28613 (2012).
134. Oliver, N., Soriano, M. C., Sukow, D. W. & Fischer, I. Dynamics of a semiconductor laser with polarization-rotated feedback and its utilization for random bit generation. *Opt. Lett.* **36**, 4632–4634 (2011).
135. Li, X.-Z. & Chan, S.-C. Heterodyne Random bit generation using an optically injected semiconductor laser in chaos. *IEEE J. Quantum Electron.* **49**, 829–838 (2013).

### Acknowledgements

M.S. acknowledges the financial support provided by Fondation Supélec, Conseil Régional de Lorraine, Agence Nationale de la Recherche (ANR) through the project TINO, grant number ANR-12-JS03-005, FEDER through the project PHOTON, and the Inter-University Attraction Pole (IAP) program of BELSPO through the project Photonics@be, grant number IAP P7/35. K.A.S. acknowledges the financial support provided by the Sêr Cymru National Research Network in Advanced Engineering and Materials.

### Additional information

Reprints and permissions information is available at [www.nature.com/reprints](http://www.nature.com/reprints). Correspondence and requests for materials should be addressed to M.S.

### Competing financial interests

The authors declare no competing financial interests.